Maximizing Production Rate and Scrub Resistance of Vinyl Acetate–VeoVa 10 Latexes

MARÍA J. UNZUÉ, AGUSTÍN URRETABIZKAIA, JOSÉ M. ASUA

Institute for Polymer Materials (POLYMAT) and Grupo de Ingeniería Química, Facultad de Ciencias Químicas, University of the Basque Country, Apartado 1072, 20080 San Sebastián, Spain

Received 30 April 1999; accepted 18 October 1999

ABSTRACT: Optimal strategies for the emulsion copolymerization of vinyl acetate and VeoVa 10 have been developed. These strategies are based on a hybrid mathematical model for the process that includes rigorous material and energy balances and empirical equations for uncertain terms. The strategies were implemented in a lab-scale calorimetric reactor. © 2000 John Wiley & Sons, Inc. J Appl Polym Sci 78: 475–485, 2000

Key words: vinyl acetate–VeoVa 10; emulsion polymerization; optimization; scrub resistance

INTRODUCTION

Vinyl acetate (VAc)–VeoVa 10 (vinyl ester of a highly branched decanoic acid, Shell Trade mark) emulsion copolymers are widely used for architectural paints, including those for indoor decoration based on highly pigmented emulsion paints [i.e., containing a high proportion of pigments plus low-cost extenders and having a pigment volume concentration (PVC) of about 80%]. These paints should be resistant to washing, which is the usual cleaning method, and hence they should have a good wet scrub resistance as determined by the standard test. The latexes required to manufacture these paints should therefore posses a high pigment-binding power in order to produce the required resistance to washing, scrubbing, and so forth.

The pigment-binding power of a latex is dependent on a number of factors. The most important of these is the average molecular weight of the latex polymer.[1] The greater the molecular weight, the higher is the pigment-binding power of the latex and, consequently, the higher the scrub resistance of the paint.[2,3]

Urretabizkaia et al.[4] studied the kinetics of the emulsion polymerization of vinyl acetate–VeoVa monomers. They reported that high molecular weight polymers can be obtained by conducting the process at low temperature and/or low initiator concentrations and/or under starved conditions, with temperature the most important factor. Unfortunately, these conditions produce long process times, resulting in low production rates. For most industrial emulsion polymerization reactors the process time is controlled (and hence the production is limited) by the heat removal rate.

The heat removal rate can be written as

$$\vartheta_1 = \mathrm{UA}(T - T_j) + \alpha(T - T_a) \qquad (1)$$

where the first term of the right-hand side member represents the heat removed through the jacket and the second term represents other heat losses (e.g., through the reactor lid); U is the overall heat transfer coefficient, which depends mostly on the viscosity of the latex, in turn depending mainly on the solids content (other contributions are agitation, particle size distribution,

Correspondence to: J. M. Asua.

Journal of Applied Polymer Science, Vol. 78, 475–485 (2000)

and so forth); A is the heat transfer area; T is the reactor temperature; T_j is the jacket temperature; T_a is the ambient temperature; and α is a heat transfer coefficient. Equation (1) shows that the heat removal rate increases linearly with the reactor temperature. In order to control the reactor temperature, the polymerization rate cannot exceed the value at which the heat generation rate equals the heat removal rate. This means process time increases as reactor temperature decreases, or in other terms, production decreases as polymer quality (molecular weight) increases. These types of problems usually present an optimal solution that is a compromise between production and product quality.

This article reports on an attempt to find the optimal strategy for the emulsion copolymerization of vinyl acetate and VeoVa 10 carried out in an industrial reactor with heat transfer limitations. The research that formed the basis for this article was organized as follows. First, a simple kinetic model for the process was developed and its parameters estimated based on experimental data. Based on this model, the optimization of the system was carried out. Finally, the optimal strategy was implemented in a lab-scale calorimetric reactor that mimicked the conditions of a large-scale reactor.

EXPERIMENTAL

Monomers, VAc, VeoVa 10, butyl acrylate (BuA), and acrylic acid were used as received. Emulsifiers [Rhodacal DS-10, $CH_3—(CH_2)_{11}—C_6H_4—SO_3Na$, Rhône–Poulenc; and Dehscofix 202, $CH_3—(CH_2)_{15–17}—(OCH_2CH_2—OH$, Albright & Wilson), initiators [sodium dithionite, 85% Fluka; potassium persulfate (KPS), 99% Fluka; sodium metabisulfite, 95% Panreac; and *tert*-butyl hydroperoxide], and buffer (potassium carbonate, 98% Panreac) were used as received. Filtered and deionized water was used throughout the work.

Polymerizations aiming at obtaining the kinetic model were carried out in a 2-L glass reactor equipped with a reflux condenser, stainless-steel stirrer, sampling device, nitrogen inlet, and feed inlet tube. Computer-driven pumps were used to feed the components of the reaction mixture into the reactor. The reactor temperature was controlled by circulating water through the reactor jacket via a thermostatic bath. A proportional-integral controller was used to maintain the desired temperature inside the reactor by manipulating the flow of cold water through a heat exchanger situated between the thermostatic bath and the reactor jacket.

Table I Recipe Used in Kinetic Runs

	Weight (g)
Initial Charge	
Anionic Surfactant (Rhodacal DS-10)	7
Sodium Dithionite	0.469
Potassium Persulfate	0.7
Solution of Monomers	34.8
Butyl Acrylate	4.2
Water	234.5
TOTAL	281.67
Initiator I Solution (Feeding time: 240 min)	
Water	362
Sodium Dithionite	1.89
Potassium Carbonate	1.12
Nonionic Surfactant (Dehscofix 202)	14
Initiator II Solution (Feeding time: 240 min)	
Water	80
Potassium Persulfate	2.8
Monomer Mixture (−34.8 g) (Feeding time: 240 min)	
VAc	492
VeoVa 10	166.1
Acrylic Acid	2.66
TBH Addition	
TBH/water	0.66/10
SMB Addition	
SMB/water	0.99/13.23
Total Solids Content: 51.2 wt %	

Table I presents the recipe used in the kinetic runs. A given amount of monomers (VAc, VeoVa 10, acrylic acid, and BuA) was dispersed in an aqueous solution of the anionic emulsifier (Rhodacal DS-10), charged into the reactor, and heated to the reactor temperature. Then an aqueous solution of the redox initiators was injected, and the initial charge was allowed to react for 10 min. The goal of this operation was to produce a seed *in situ*. In this operation only anionic emulsifier was used because nonionic emulsifiers are less effective for particle nucleation, presumably due to their low diffusion coefficient, a result of their large size.[5] On the other hand, a small amount of BuA was used because it has been observed that polymerization of vinyl esters starts much more readily in the presence of a small amount of BuA.[6]

Table II Summary of Kinetic Runs Carried Out

Run	T (°C)	wt % KPS[a]	wt % E[b]
1	50	0.50	3
2	65	0.50	3
3	80	0.50	3
4	65	0.25	3
5	80	0.25	3
6	65	0.125	3
7	80	0.125	3

[a] wt % of KPS based on total monomer, with KPS/SDT as constant.
[b] wt % of total emulsifier based on total monomer.

In the semicontinuous operation the feed was divided into three streams. The first was an aqueous solution of sodium dithionite, potassium carbonate, and the nonionic emulsifier (Dehscofix 202). The second was an aqueous solution of potassium persulfate, and the third a mixture of monomers (VAc, VeoVa 10, and acrylic acid). The feeding time was 4 h. At the end of the feeding, the reactor temperature was increased (if needed) to 80–90°C, and aqueous solutions of sodium metabisulfite and *tert*-butyl hydroperoxide were separately fed to the reactor during a 30-min period to reduce the residual monomer. The whole process was carried out under a nitrogen blanket. Table II summarizes the kinetic runs.

Samples were withdrawn from the reactor at appropriate intervals, and the polymerization was shortstopped with hydroquinone. The conversion was determined gravimetrically. The particle size of the latexes was measured by dynamic light scattering (Malvern 4700). This value together with that of the overall conversion was used to estimate the number of polymer particles. The molecular weight distribution was analyzed by gel-permeation chromatography (Waters 510), comparing the results with polystyrene standards and the required correction factors of the variation of the refractive index with the concentration.

The optimal strategies were implemented in a lab-scale reactor calorimeter (RC1, Mettler). Agitation was provided by an anchor stirrer. Oxygen was removed from the reactor by purging with nitrogen. To obtain the evolution of the monomer conversion, it is not necessary to collect data, as this can be estimated from the calorimetric measurements. The heat balance is:

$$(m_r cp_r + \Sigma m_j cp_j)\frac{dT}{dt} = Q_g - Q_h - Q_f + Q_s + Q_c - Q_1 \quad (2)$$

where the left-hand side term represents the heat accumulated in the reactor, Q_g is the heat generation rate due to polymerization, Q_h is the heat flux across the reactor wall, Q_f is the heat due to the feeds, Q_s and Q_c represent the heating due to stirring and the calibration heater, respectively, and Q_1 represents the heat loss to the surroundings. Calculating polymerization heat from the other terms—the essence of reaction calorimetry—can be done if the terms can be determined with sufficient accuracy. The equipment used allows for an accurate estimation of all terms in eq. (2).[7–9] The polymerization rate, Rp, is calculated as follows:

$$Rp = \frac{Q_g}{\int_0^{tf} Q_g\, dt} X_{tf} M_T \quad (3)$$

where X_{tf} is the overall monomer conversion at the end of the reaction (which is measured by gravimetry) and M_T is the total amount of monomer in the formulation. The evolution of the overall conversion is calculated as

$$X_t = \frac{\int_0^{t} Q_g\, dt}{\int_0^{t_f} Q_g\, dt} X_{tf} \quad (4)$$

The fractional conversion, X, is calculated by means of the following equation:

$$X = \frac{X_t M_T}{\int_0^{t} F_M\, dt} \quad (5)$$

where F_M is the total monomer feed rate.

RESULTS AND DISCUSSION

Figure 1 shows the effect of the reactor temperature on the evolution of the fractional conversion

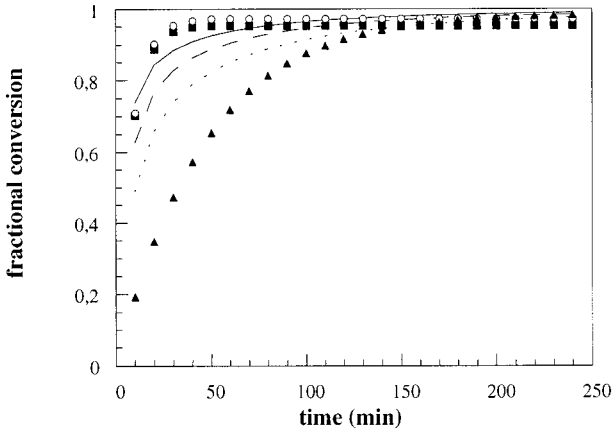

Figure 1 Effect of the reactor temperature on the evolution of the fractional conversion; amount of initiator is 0.5 wt %. Legend: 50°C (▲, · · · · · ·); 65°C (○, - - - -); 80°C (■, —). Points are experimental data, lines are model predictions.

of the monomers for an initiator concentration (in terms of KPS) of 0.5 wt %. It can be seen that monomer conversion significantly increased when the reactor temperature increased from 50°C to 65°C, leading to a highly starved process. Additional increases of the reactor temperature (to 80°C) did not yield higher conversions. Figure 2 presents the evolution of the number of polymer particles during the polymerizations carried out at different temperatures with a 0.5 wt % of initiator. It can be seen that a large number of polymer particles was initially formed, but a continuous limited coagulation occurred throughout the

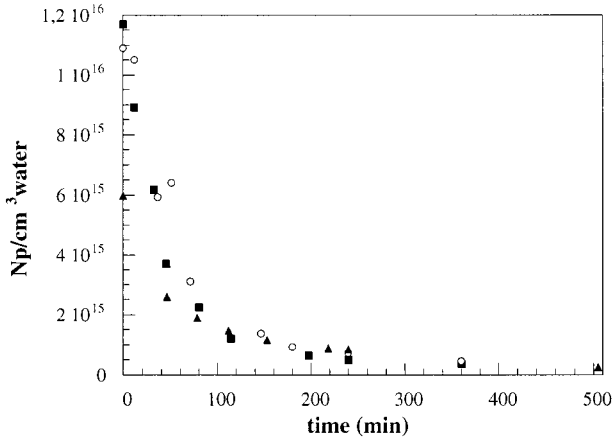

Figure 2 Effect of the reactor temperature on the evolution of the number of particles per cm⁻3; amount of initiator is 0.5 wt %. Legend: 50°C (▲); 65°C (○); 80°C (■).

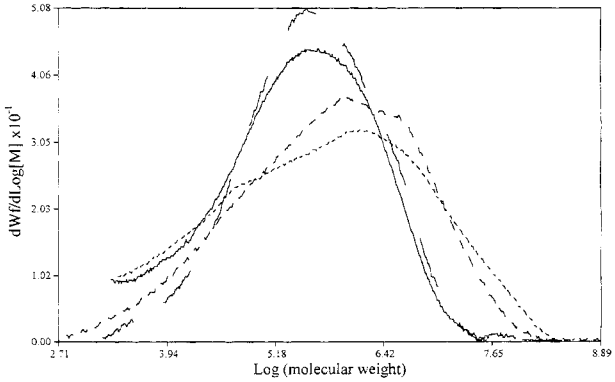

Figure 3 Evolution of the molecular weight distributions during run 1 (T = 50°C). Legend: 11 min (—); 50 min (– – –); 153 min (- - - -); 505 min (· · · · · ·).

process, leading to a substantial decrease of the number of polymer particles. Note that no macroscopic coagulum was observed. Figure 2 also shows that although the initial number of polymer particles increased with temperature, the final number was independent of temperature.

Figure 3 presents the evolution of the molecular weight distribution (MWD) during run 1 (50°C). It can be seen that the molecular weight distribution increased during the process. This increase was the result of the appearance of a high molecular peak, a likely outcome of the chain transfer to polymer that occurred in the second part of the process (once high fractional conversions were reached; see Fig. 1). Figure 4 shows that effect of the reactor temperature on the MWD. It can be seen that the higher the temperature, the lower the molecular weight. Figure 5 shows the correlation between the weighted-aver-

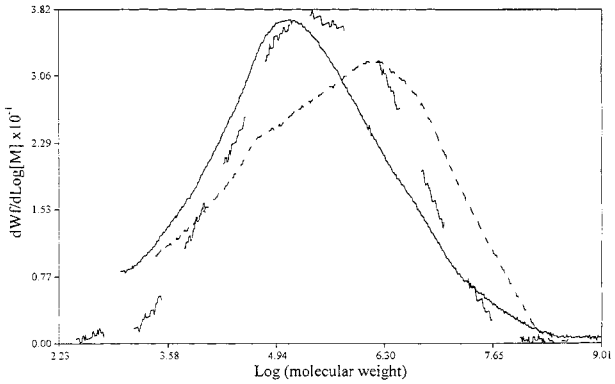

Figure 4 Effect of the reactor temperature on the MWD; amount of initiator is 0.5 wt %. Legend: 50°C (- - - -); 65°C (– – –); 80°C (—).

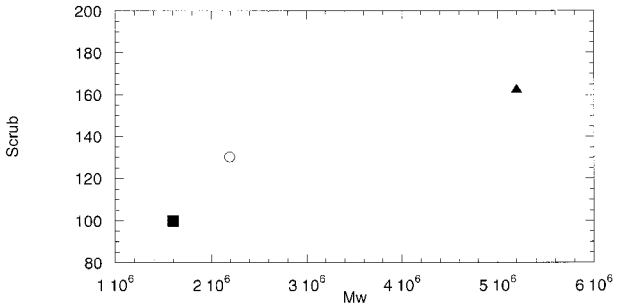

Figure 5 Effect of $\bar{M}_w$ on the scrub resistance in arbitrary units: (▲) run 1, 50°c; (○) run 2, 65°C; (■) run 3, 80°C.

age molecular weight and scrub resistance. Note that the higher the molecular weight, the higher the scrub resistance.

Figure 6 presents the effect of the reactor temperature on monomer conversion for the polymerizations carried out with a 0.25 wt % of initiator. It can be seen that conversion increased with temperature (in particular during the first stages of the process). The number of polymer particles (not shown) presented an evolution similar to that of Figure 2, and the final value was independent of the reactor temperature. It was found that molecular weight decreased as temperature increased. Similar results were found with 0.125 wt % of initiator.

Figures 7, 8, and 9 present the effect of the initiator concentration on monomer conversion, number of polymer particles, and MWD of the

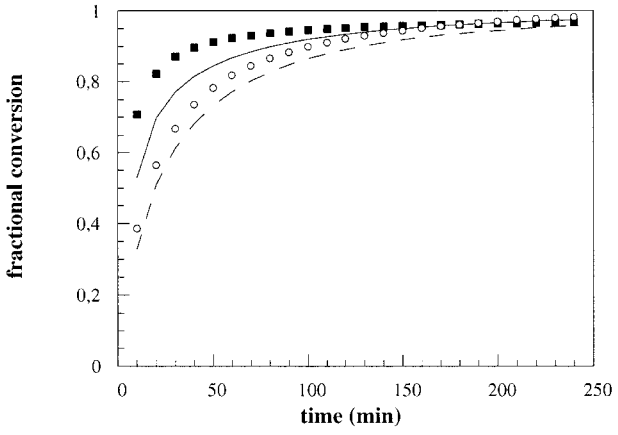

Figure 6 Effect of the reactor temperature on the evolution of the fractional conversion; amount of initiator is 0.25 wt %. Legend: 65°C (○, - - - -); 80°C (■, —). Points are experimental data and lines are model predictions.

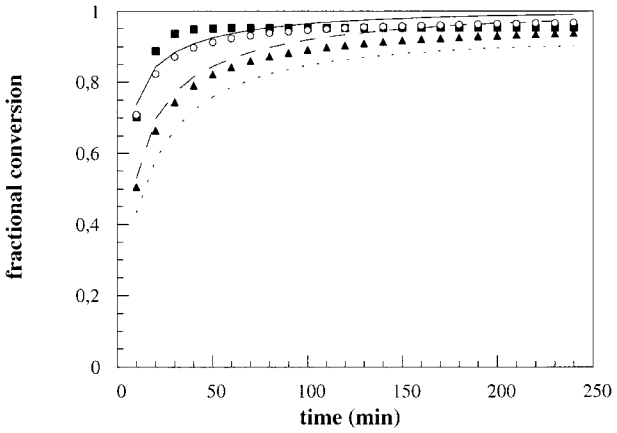

Figure 7 Effect of the amount of initiator on the evolution of the fractional conversion; temperature is 80°C. Legend: 0.50 wt % initiator (■, —); 0.25 wt % initiator (○, – – –); 0.125 wt % initiator (▲, - - - -). Points are experimental data and lines are model predictions.

final latex, respectively, at 80°C. It can be seen that monomer conversion increased with initiator concentration. A more surprising result was the decrease in the number of polymer particles when the initiator concentration increased. In principle, it would be expected that the number of polymer particles would increase with the initiator concentration because the nucleation rate increased with the number of radicals generated, that is, with the initiator concentration. Actually, this was observed for the samples taken after the polymerization of the initial charge (experimental

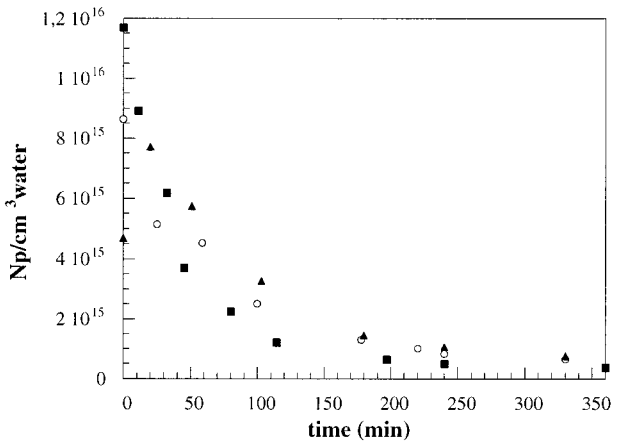

Figure 8 Effect of the amount of initiator on the evolution of the number of polymer particles per cm^3 of water; temperature is 80°C. Legend: 0.50 wt % initiator (■); 0.25 wt % initiator (○); 0.125 wt % initiator (▲).

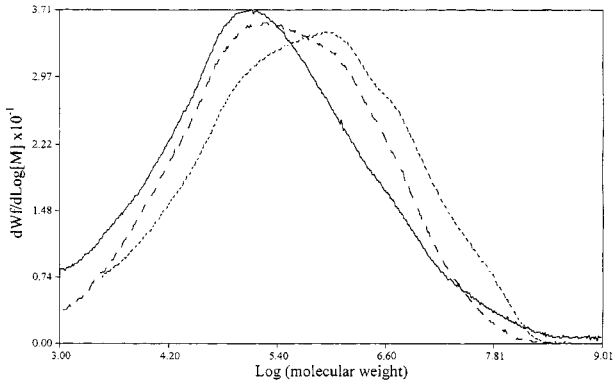

Figure 9 Effect of the amount of initiator on the MWD of the final latex; temperature is 80°C. Legend: 0.50 wt % initiator (—, scrub 100%); 0.25 wt % initiator (– – –, scrub 140%); 0.125 wt % initiator (· · · · · ·).

points at t = 0 in Fig. 8). However, Figure 8 shows that, during the semicontinuous process, coagulation was more severe for high initiator concentrations, behavior resulting from increasing ionic strength with the initiator concentration and therefore the resulting decrease in the efficiency of the emulsifier system (which includes an anionic emulsifier).[10–13] Figure 9 shows that the molecular weight increased when the initiator concentration decreased. The relative number of scrub cycles of these samples is given in this figure's caption. It can be seen that the scrub resistance increased with the molecular weight of the polymer. Similar results were obtained at other temperatures.

Mathematical Modeling

Although process optimization may be carried out experimentally using a trial-and-error method, this is a very expensive and time-consuming process that, in addition, does not guarantee the reaching of an optimal solution. Using standard optimization techniques based on a mathematical model for the process is a much better approach. There is a very rich literature about mathematical modeling of emulsion polymerization systems.[14–20] These models provide a useful framework to develop models for particular systems. However, this is not a trivial task because this framework includes alternative mechanisms (e.g., heterogeneous,[21] homogeneous,[22] and coagulative nucleation,[23–27] and it is very difficult to predict accurately which one is operative for a particular case. On the other hand, the models contain a large number of parameters that cannot be accurately predicted and are difficult to estimate from independent measurements.[28,29] Not unexpected is the limited predictive ability of emulsion polymerization models, in particular for systems such as the present one, in which technical (containing inhibitors), nontraditional monomers (VeoVa 10) are used in formulations that contain mixed emulsifier systems and redox initiators.

Therefore, it was decided to use a hybrid model that included rigorous material balances for the monomers and molecular weights and empirical functions for the uncertain terms.

The monomer balances are

$$\frac{di_T}{dt} = -\left(\sum_j kp_{ji}P_j\right)[i]_p \frac{\bar{n}Np}{N_A} + Fi \quad \text{(mol/s)} \tag{6}$$

where i_T is the total number of moles of monomer i in the reactor, kp_{ji} the propagation rate constant, P_j the probability of finding a radical with ultimate unit of type i,[30,31] $[i]_p$ the concentration of monomer i in the polymer particles, $\bar{n}$ the average number of radicals per particle, Np the total number of polymer particles in the reactor, N_A Avogadro's number, and Fi the feed rate of monomer i.

As the reactivity ratios of the main monomers are close to unity, eq. (1) was approximated by

$$\frac{dM}{dt} = -k_{pVAc}[M]_p\frac{\bar{n}Np}{N_A} + F_M \quad \text{(mol/s)} \tag{7}$$

where M is the total amount of monomer in the reactor, k_{pVAc} the propagation rate of the vinyl acetate, and $[M]_p = [i]_p$ and $F_M = \Sigma F_{io}$. Any error caused by this approximation is transferred to $\bar{n}xNp$ and compensated by the estimation procedure, as shown below.

The balance of the cumulative weighted-average molecular weight, $\overline{M}_w$, is given by

$$\frac{d\overline{M}_w}{dt} = \frac{1}{X_T}(\overline{M}_{w_{\text{inst}}} - \overline{M}_w)\frac{dX_T}{dt} \tag{8}$$

where X_T is the overall monomer conversion defined as the ratio between the amount of monomer converted to polymer and the total amount of monomer in the recipe; and $\overline{M}_{\text{winst}}$ is the instantaneous weighted-average molecular weight.

Table III Values of Parameters

Parameter	Value 10^{16}	Parameter	Value 10^{-3}
a1	−8.540	b1	0.d0
a2	4.382	b2	0.400
a3	6.395	b3	5.867
a4	−8.978	b4	−1.261
a5	−24.76	b5	−5.583
a6	35.33	b6	6.265
a7	99.66	b7	−2.909
a8	83.25	b8	−5.193
a9	16.40	b9	−2.836
a10	19.13	b10	−5.869
a11	−90.19	b11	−2.361
a12	30.00		
a13	−23.80		
$k^0_{p_{VAc}} = 3.2 \times 10^{-10}$ (cm^3 mol^{-1} s^{-1}) [32]			
$E_{VAc} = 6.3$ (kcal mol^{-1}) [32]			
$r_A = r_B = 1$			

The uncertainties associated with eqs. (7) and (8) are due to $\tilde{n}$, N_p, and $\overline{M}_{winst}$. Therefore, it was decided to develop empirical equations for $\tilde{n}xNp$ and $\overline{M}_{winst}$. There are several alternatives for these empirical equations including polynomials, neural networks, and fuzzy logic models. In this work polynomials were used. It was assumed that $\tilde{n}xNp$ depended on the relative time, *tr,* (actual time/time required to complete monomer addition); the initiator feed rate, q_I(implicit is the assumption that the redox initiator reacts instantaneously); and temperature, T.

$$\bar{n}xNp = a_1 + a_2 tr + a_3 q_I + a_4 T + a_5 tr q_I + a_6 trT + a_7 q_I T + a_8 tr^2 + a_9 tr^2 T + a_{10} q_I^2 tr + a_{11} q_I^2 T + a_{12} T^2 tr + a_{13} T^2 q_I \quad (9)$$

On the other hand, it was assumed that the instantaneous weight-average molecular weight depended on the initiator feed rate (the higher the q_I, the lower the $\overline{M}_{winst}$); the reactor temperature (the higher the T, the lower the $\overline{M}_{winst}$); and the fractional conversion according to the following equation:

$$\overline{M}_{winst} = b_1 + b_2 x_j + b_3 q_I + b_4 T + b_5 x_j q_I + b_6 x_j T + b_8 x_j^2 q_I + b_9 x_j^2 T + b_{10} q_I^2 x + b_{11} q_I^2 T \quad (10)$$

The fractional conversion accounts for both the propagation rate per active polymer chain (which increases when x_j decreases, i.e., when the monomer concentration in the polymer particles increases) and the chain transfer reaction to polymer (which increases when x_j increases, i.e., when the polymer concentration in the polymer particles increases). An increase of the propagation rate leads to an increase of the molecular weights. Also an increase of the chain transfer to polymer causes an increase in the molecular weights as branched polymer is formed.

The parameters of the polynomials defined by eqs. (9) and (10) were estimated by minimizing the following objective functions:

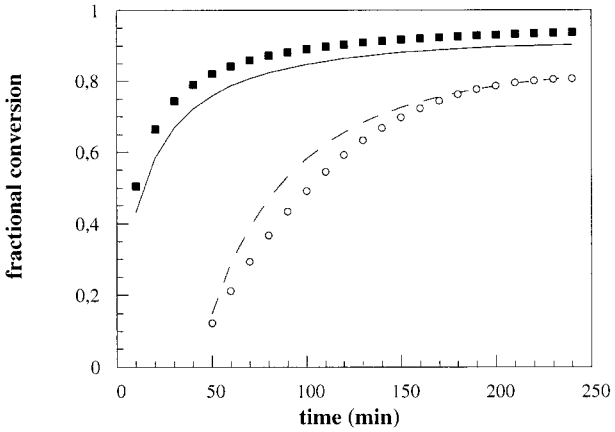

Figure 10 Effect of the amount of initiator on the evolution of the fractional conversion; amount of initiator is 0.125 wt %. Legend: 65°C (○, - - - -); 80°C (■, —). Points are experimental data and lines are model predictions.

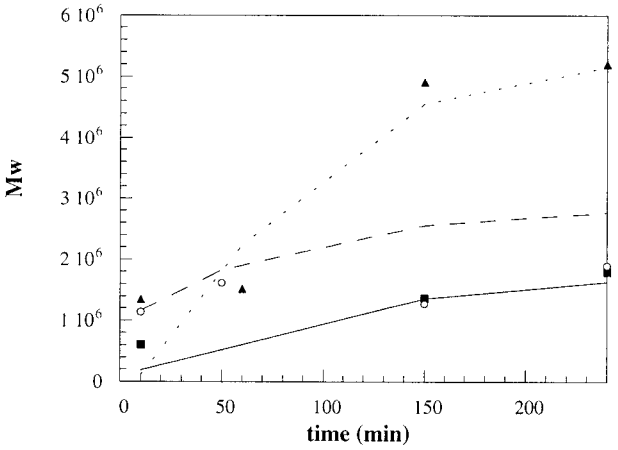

Figure 11 Effect of the amount of initiator on the evolution of the $\bar{M}_w$; amount of initiator is 0.50 wt %. Legend: 50°C (▲, - - - -); 65°C (○, – – –); 80°C (■, —). Points are experimental data and lines are model predictions.

$$J_1 = \sum_{h=1}^{z_1} \sum_{k_T=1}^{z_2(h)} [(X_j)_{\exp} - X_j]^2 \tag{11}$$

$$J_2 = \sum_{h=1}^{z_1} \sum_{k=1}^{z_2(h)} [(\bar{M}_w)_{\exp} - \overline{M}_w]^2 \tag{12}$$

where z_1 is the number of runs, $z_2(h)$ the number of measurements in run h, and the subscript "exp" stands for experimentally measured values. Table III presents the estimated values of the parameters as well as the values of the parameters in eq. (1) taken from literature.

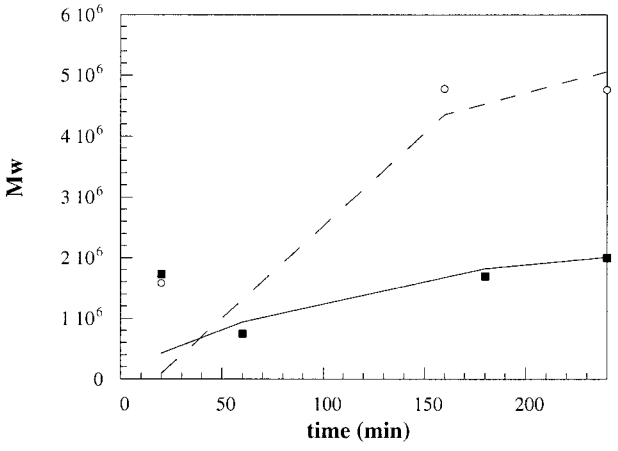

Figure 12 Effect of the amount of initiator on the evolution of the $\bar{M}_w$; amount of initiator is 0.25 wt %. Legend: 65°C (○, – – –); 80°C (■, —). Points are experimental data and lines are model predictions.

Table IV Reactor Characteristics and Heat Balance Parameters

Volume:	15 m^3
Weight (m_r):	3×10^3 kg
T_0:	20°C
T_j:	20°C
T_s:	20°C
Q_{rc}:	0
$(-\Delta H)$:	87.9 kJ mol^{-1}

Figures 1, 6, 7, and 10 present a comparison between the experimental results and the model predictions for the evolution of the fractional conversion, for which the figures showed a good agreement. There was also good agreement between the evolution of the weighted-average molecular weights predicted by the model with those measured experimentally, which are compared in Figures 11 and 12.

Process Optimization

The goal was to maximize both the production rate and the scrub resistance of the paint made out of the latex. Maximization of the production rate is equivalent to minimizing the process time. On the other hand, Figure 5 shows that the scrub resistance increased with the molecular weight. With these ideas in mind, the objective function to be minimized was:

$$J_3 = \frac{10^6}{\overline{M}_w} + t_j \times 10^{-4} \tag{13}$$

where t_j is the feeding time in seconds. The weighing factors (10^6 and 10^{-4}) were chosen to give similar importance to production and product quality. Obviously, other choices can be used.

A 15-m^3 industrial reactor was considered. The characteristics of the reactor are given in Table IV. In order to carry out the optimization, material and energy balances are needed. The material balance for the monomer and the balance for $\bar{M}_w$ are given by eqs. (2) and (3), respectively. The material balance for water is:

$$\frac{dw}{dt} = q_w \quad \text{(kg/s)} \tag{14}$$

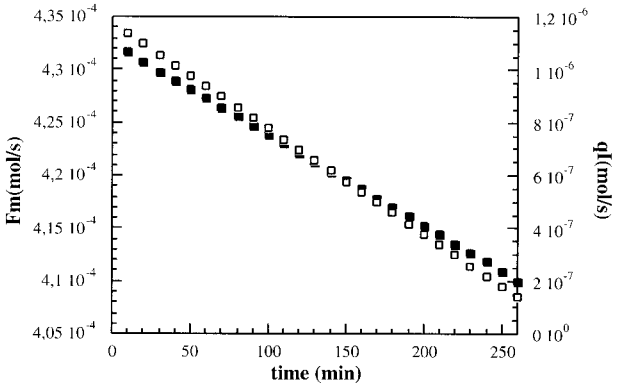

Figure 13 Optimal monomer (■) and initiator (□) feed flow rates calculated for Case I.

The energy balance was:

$$(m_r c_{pr} + \sum m_k cp_k)\frac{dT}{dt} = k_{p\mathrm{VAc}}[M]_p \frac{\bar{n}N_p}{N_A}(-\Delta H) - UA(T - T_j) - Q_{rc} + \sum F_i C_{pi}(T_0 - T) - \alpha(T - T_s) \quad (15)$$

where m_r is the reactor weight, c_{pr} its specific heat capacity, m_k the amount of compound k in the reactor, cp_k its specific heat capacity, $(-\Delta H)$ the heat of polymerization, U the overall heat transfer coefficient, A the heat transfer area, T_j the temperature of the jacket, Q_{rc} the heat transfer in the reflux condenser, F_i the feed rate of compound i, α a heat transfer coefficient accounting for heat losses other than through the jacket, and T_s the temperature of the surroundings.

In addition, the following constraints were considered:

(1) The monomer conversion at the end of the monomer addition must be higher than 0.92 (to reduce the time of the postpolymerization process needed for the minimization of the residual monomer).
(2) The fractional conversion during the process should be less than 0.96. (This is a constraint associated with the accuracy of the model because it was developed based on data collected at fractional conversions lower than 0.96, and it is uncertain to extrapolate polynomials.
(3) The reactor temperature should be lower than 80°C to minimize monomer boiling.
(4) The compounds already added into the reactor could not be removed.

$$F_M \geq 0 \quad (16)$$

$$q_I \geq 0 \quad (17)$$

$$q_w \geq 0 \quad (18)$$

(5) The initial temperature of the process was set equal to 20°C. The rationale behind this is that heating the reactor before polymerization takes time, is expensive, and results in a lower molecular weight polymer because a higher average temperature was used in the process. Starting the process at a low temperature allows for the process to be conducted at a lower average temperature but with higher polymerization rates because the excess of heat is used to increase the reactor temperature.

The optimization variables used to minimize the objective function given by eq. (13) were the feed rates of the mixture of monomers and initiator and the total amount of initiator used.

Two cases were considered. In Case I rather severe heat transfer limitations were used:

$$UA = 3.37\mathrm{kJs^{-1}{}^{\circ}C^{-1}} \quad (19)$$

$$\alpha = 1.30\mathrm{kJs^{-1}{}^{\circ}C^{-1}} \quad (20)$$

Notice that for convenience UA was kept constant during the process. In general, U decreases (because the solids content increases and hence the viscosity increases) and A increases (because the volume of the reaction mixture increases). The evolution of UA depends on the way in which the

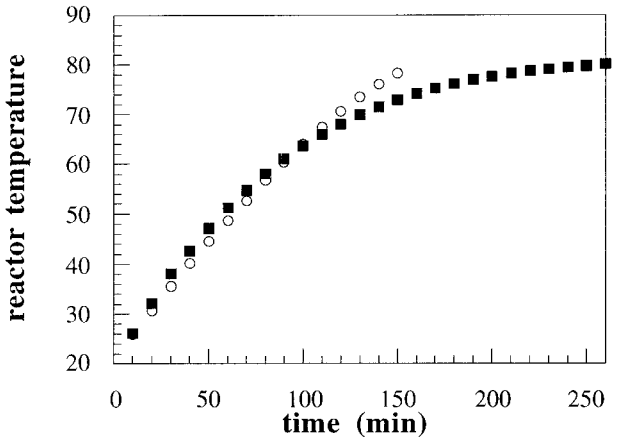

Figure 14 Reactor temperature predicted by the model for Case I (■) and Case II (○).

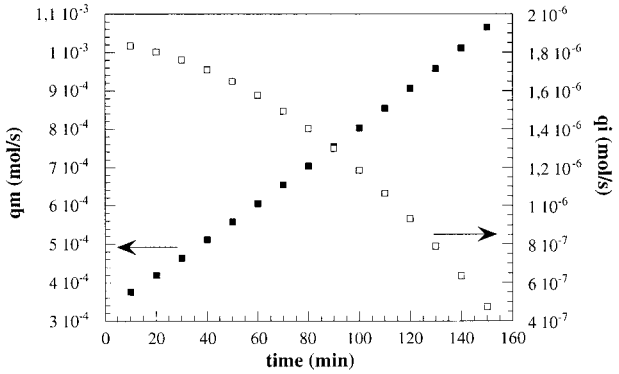

Figure 15 Optimal monomer (■) and initiator (□) feed rates for Case II.

process is carried out. Thus, in a system in which the solids content does not increase significantly because preemulsified monomers are added, *UA* may be roughly constant or even decrease slightly. If a neat monomer addition is used, a substantial decrease of *UA* is expected because of the increase of the latex viscosity. It has to be pointed out that this method is not limited to a constant value of *UA*. Linear addition profiles of the mixture of monomers and initiator were used:

$$F_M = c_1 + c_2 t \tag{21}$$

$$q_I = d_1 + d_2 t \tag{22}$$

The parameters as well as the total amount of initiator were estimated by minimizing the objective function given in eq. (13) by means of a direct search algorithm (subroutine DBCPOL, IMSL library). Figure 13 presents the feed profiles of the mixture of monomers and initiator (scaled down for a 1.5-L reactor) and Figure 14 the temperature profile calculated by the model for Case I.

Table V Scrub Resistances of Paints Prepared with Different Latexes

Run	Temperature (°C)	Scrub Resistance (Relative to Latex in Run 3)
1	50	163%
3	80	100%
Case I	profile	143%
Case II	profile	150%

In Case II better thermal characteristics were considered:

$$UA = 6.74\text{kJs}^{-1}\text{°C}^{-1} \tag{23}$$

$$\alpha = 2.60\text{kJs}^{-1}\text{°C}^{-1} \tag{24}$$

and parabolic addition profiles of the mixture of monomers and initiator were used:

$$F_M = c_1 + c_2 t + c_3 t^2 \tag{25}$$

$$q_I = d_1 + d_2 t + d_3 t^2 \tag{26}$$

Figure 15 presents the feed profiles obtained (scaled down for a 1.5-L reactor) and Figure 14 the evolution of temperature calculated by the model for Case II. Comparing these results with those obtained in Case I, it can be seen that with higher heat removal rate a significant reduction of the process time in the reactor was achieved. The optimal strategies were implemented in a lab-scale reactor calorimeter (RC1, Mettler). The mix-

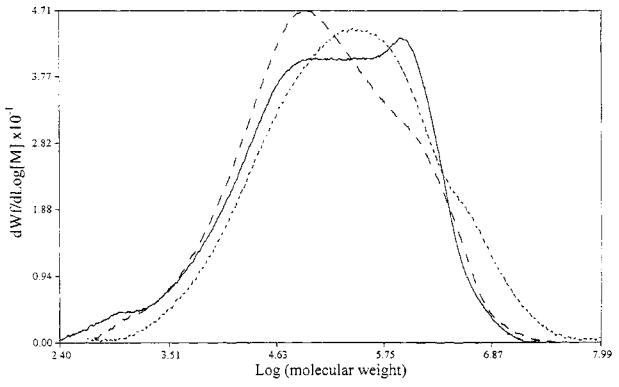

Figure 16 Comparison between the MWD obtained in the optimal process with those obtained at a constant temperature. Legend: Case I (—); 50°C (· · · · · ·); 80°C (– – –).

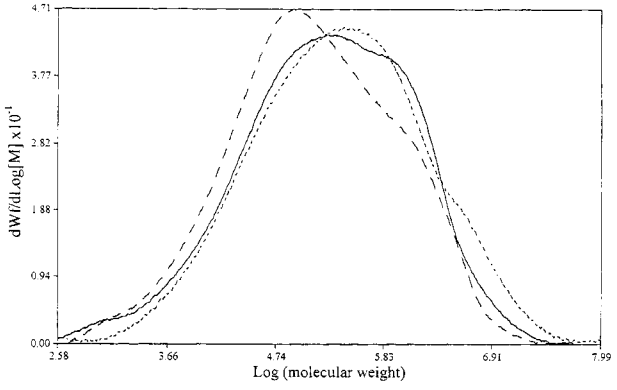

Figure 17 Comparison between the MWD obtained in the optimal process with those obtained at a constant temperature. Legend: Case II (—); 50°C (· · · · · ·); 80°C (– – –).

ture of monomers and initiator, following the profiles given in Figures 13 and 15, were fed into the reactor by means of computer-driven pumps. The temperature was forced to follow the profiles presented in Figure 14. Figure 16 shows the molecular weight distribution of the final latex for Case I as well as those obtained in the isothermal processes carried out at 50°C (run 1) and 80°C (run 3). It can be seen that the MWD obtained in the optimal process is similar to that obtained at 50°C and higher than that produced at 80°C. Table V shows a higher scrub resistance of the paint prepared with the latex obtained in Case I than that of the latex obtained at 80°C and a slightly smaller resistance than that obtained with the latex prepared at 50°C.

Figure 17 compares the MWD obtained in Case II with those of the latex prepared at 50°C and 80°C. The MWD obtained in the optimal process was similar to that obtained at 50°C and higher than that produced at 80°C. The scrub resistance is similar to that of the latex produced under isothermal conditions at 50°C, but the process time was reduced by 40%.

CONCLUSIONS

This article has reported on an attempt to find the optimal strategy for the emulsion copolymerization of vinyl acetate and VeoVa 10 in order to maximize the production rate and scrub resistance of latexes produced in reactors with a limited capacity to remove heat. The effect of the operation variables on the kinetics of the process was studied and a hybrid mathematical model for the process developed. The model included rigorous material and energy balances, as well as empirical functions for the uncertain terms ($\tilde{n}xN_p$ and $\bar{M}_{w\text{inst}}$). The model fit the experimental results well. As scrub resistance increased with the molecular weight of the polymer, an optimization seeking minimum process time and maximum molecular weight was performed. Weighing factors were used in the objective function to give similar importance to production and product quality. The optimal strategies were implemented in a lab-scale calorimetric reactor. It was found that a 40% reduction in the process time can be achieved while still maintaining product quality.

REFERENCES

1. VeoVa Technical Manual 3.3, Shell, 1988.
2. Aten, W. C. Technical Report TN-R 84-04, Shell.
3. Vermeulen Technical Report TN-R 84-01, Shell.
4. Urretabizkaia, A.; Unzué, M. J.; Asua, J. M.; Arzamendi, G., manuscript in preparation.
5. Dunn, A. S. Polymer International 1993, 30, 547.
6. Unzué, M. J.; Asua, J. M., manuscript in preparation.
7. Gugliotta, L. M.; Arotçarena, M.; Leiza, J. R.; Asua, J. M.; Polymer 1995, 36, 2019.
8. Gugliotta, L. M.; Leiza, J. R.; Arotçarena, M.; Armitage, P. D.; Asua, J. M.; Ind Eng Chem Res 1995, 34, 3899.
9. Sáenz de Buruaga, I.; Armitage, P. D.; Leiza, J. R.; Asua, J. M.; Ind Eng Chem Res 1997, 36, 4243.
10. Goodwin, J. W.; Hearn, J.; Ho, C.C.; Ottewill R. H. Br Polym J 1973, 5, 347.
11. Dunn, A. S. In Emulsion Polymerization of Vinyl Acetate; El-Aasser, M. S.; Vanderhoff, J. W., Eds.; Applied Science Publishers: London, UK, 1981.
12. Zollars, R. L. In Emulsion Polymerization of Vinyl Acetate; El-Aasser, M. S.; Vanderhoff, J. W., Eds.; Applied Science Publishers: London, UK, 1981.
13. Shouldice, G. T. D.; Vandezande, G. A.; Rudin, A. Env Polym J 1994, 30, 179.
14. Min, K. W.; Ray, W. H. J Macromol Sci Rev Macromol Chem Phys 1974, C11, 177.
15. Penlidis, A.; MacGregor, J. F.; Hamielec, A. E. In Computer Applications in the Polymer Laboratory; Prodver, T., Ed.; ACS Symposium Series, ACS: Washington, 1986, p 219.
16. Omi, S.; Kushibiki, K.; Iso, M. Polym Eng Sci 1987, 27, 470.
17. Urretabizkaia, A.; Arzamendi, G.; Asua, J. M.; Chem Eng Sci 1992, 47, 2579.
18. Arzamendi, G.; Asua, J. M. Macromolecules 1995, 28, 7479.
19. Dube, M.; Soares, J. B. P.; Penlidis, A.; Hamielec, A. E. Ind Eng Chem Res 1997, 36, 966.
20. Saldivar, E.; Dafniotis, P.; Ray, W. H. J Macromol Sci Rev. Macromol Chem Phys 1998, C38, 207.
21. Smith, W. V.; Ewart, R. H. J Chem Phys 1948, 16, 592.
22. Roe, C. P. Ind Eng Chem 1968, 60, 20.
23. Fitch, R. M.; Tsai, C. H. In Polymer Colloids; Fitch, R. M., Ed.; Plenum Press: New York, 1973.
24. Hansen, F. K.; Ugelstad, J. J Polym Sci, Polym Chem Ed 1978, 16, 1953.
25. Hansen, F. K.; Ugelstad, J. J Polym Sci, Polym Chem Ed 1979, 17, 3033.
26. Hansen, F. K.; Ugelstad, J. J Polym Sci, Polym Chem Ed 1979, 17, 3047.
27. Richards, J. R.; Congalidis, J. P.; Gilbert, R. G. J Appl Polym Sci 1989, 37, 2727.
28. López de Arbina, L.; Barandiaran, M. J.; Asua, J. M. Polymer 1997, 37, 5907.
29. López de Arbina, L.; Barandiaran, M. J.; Asua, J. M. Polymer 1997, 38, 143.
30. Forcada, J.; Asua, J. M. J Polym Sci, Polym Chem Ed 1985, 23, 1955.
31. Arzamendi, G.; de la Cal, J. C.; Asua, J. M., Angew Makromol Chem 1992, 194, 47.
32. Walling, C. Free Radical Polymerization in Solution; Wiley-Interscience: New York, 1957.